

OBSERVATIONS OF SOLAR ENERGETIC PARTICLES FROM ^3He -RICH EVENTS OVER A WIDE RANGE OF HELIOGRAPHIC LONGITUDE

M. E. WIEDENBECK¹, G. M. MASON², C. M. S. COHEN³, N. V. NITTA⁴, R. GÓMEZ-HERRERO^{5,6}, AND D. K. HAGGERTY²

¹ Jet Propulsion Laboratory, California Institute of Technology, Pasadena, CA 91109, USA; mark.e.wiedenbeck@jpl.nasa.gov

² Applied Physics Laboratory, Johns Hopkins University, Laurel, MD 20723, USA

³ Space Radiation Laboratory, California Institute of Technology, Pasadena, CA 91125, USA

⁴ Lockheed-Martin Solar and Astrophysics Lab, Palo Alto, CA 94304, USA

⁵ Christian-Albrechts Universität zu Kiel, D-24118 Kiel, Germany

Received 2012 September 25; accepted 2012 November 6; published 2012 December 14

ABSTRACT

A prevailing model for the origin of ^3He -rich solar energetic particle (SEP) events attributes particle acceleration to processes associated with the reconnection between closed magnetic field lines in an active region and neighboring open field lines. The open field from the small reconnection volume then provides a path along which accelerated particles escape into a relatively narrow range of angles in the heliosphere. The narrow width (standard deviation $<20^\circ$) of the distribution of X-ray flare longitudes found to be associated with ^3He -rich SEP events detected at a single spacecraft at 1 AU supports this model. We report multispacecraft observations of individual ^3He -rich SEP events that occurred during the solar minimum time period from 2007 January through 2011 January using instrumentation carried by the two Solar Terrestrial Relations Observatory spacecraft and the *Advanced Composition Explorer*. We find that detections of ^3He -rich events at pairs of spacecraft are not uncommon, even when their longitudinal separation is $>60^\circ$. We present the observations of the ^3He -rich event of 2010 February 7, which was detected at all three spacecraft when they spanned 136° in heliographic longitude. Measured fluences of ^3He in this event were found to have a strong dependence on longitude which is well fit by a Gaussian with standard deviation $\sim 48^\circ$ centered at the longitude that is connected to the source region by a nominal Parker spiral magnetic field. We discuss several mechanisms for distributing flare-accelerated particles over a wide range of heliographic longitudes including interplanetary diffusion perpendicular to the magnetic field, spreading of a compact cluster of open field lines between the active region and the source surface where the field becomes radial and opens out into the heliosphere, and distortion of the interplanetary field by a preceding coronal mass ejection. Statistical studies of additional ^3He -rich events detected at multiple spacecraft will be needed to establish the relative importance of the various mechanisms.

Key words: interplanetary medium – Sun: flares – Sun: particle emission

Online-only material: color figures

1. INTRODUCTION

Solar energetic particles (SEPs) are commonly thought to arise from two distinct acceleration mechanisms: in “gradual” SEP events, shocks driven by coronal mass ejections (CMEs) are responsible for energizing the particles while in “impulsive” SEP events, the acceleration is driven by magnetic reconnection. Various tabulations of the characteristics distinguishing the two types of events have been attempted (e.g., Reames 1999; Mewaldt et al. 2007a). While abundance ratios in gradual events typically resemble those in coronal or solar wind material to within factors $\lesssim 2$ (Mewaldt et al. 2007b), impulsive events are characterized by enhancements of $^3\text{He}/^4\text{He}$ up to at least 10^3 , leading to the designation of “ ^3He -rich” for these events. In addition, impulsive events often have the ratio Fe/O enhanced by factors ~ 10 and are frequently accompanied by near-relativistic electron events with electron-to-proton ratios significantly greater than typically observed in gradual SEP events.

Individual gradual events are observed over a wide range of heliographic longitudes, which is attributed to the injection of accelerated particles on a wide range of magnetic field lines as the shock intersects these field lines near the Sun. In contrast,

in impulsive events, the spatially compact acceleration region should give energetic particles access only to a small cluster of open field lines involved in the reconnection (Shimojo & Shibata 2000; Reames 2002). The relatively narrow range of heliographic longitudes occupied by this group of field lines at 1 AU is thought to be responsible for the reported narrow longitudinal extent of ^3He -rich events.

The primary observational evidence for the narrow longitudinal spread of impulsive SEPs has come from studies in which ^3He -rich events were detected at a spacecraft located near 1 AU and the injection of the particles at the Sun could be temporally associated with an X-ray flare (Reames et al. 1998; Reames 1993, 1999). The distribution of heliographic longitude differences between the spacecraft and the flare was found to have a mean value corresponding to that expected for a Parker-spiral magnetic field for a velocity of $\sim 400 \text{ km s}^{-1}$, which is typical of the slow solar wind. Reames (1999) reported an approximately Gaussian distribution of longitudinal offsets with a standard deviation in the range 15° – 20° and noted that much of this could be attributed to event-to-event differences in the solar wind speed, which determines how tightly the Parker spiral is wound.

There have been a few studies of the longitudinal breadth of individual impulsive SEP events observed at multiple spacecraft. Data from the two *Helios* spacecraft were used in conjunction with observations from near-Earth spacecraft to look for correlated detections of energetic electrons (Wibberenz &

⁶ Present affiliation: Space Research Group, University of Alcalá, E-28871 Alcalá de Henares, Spain.

Cane 2006) or ^3He (Reames & Stone 1986; Reames et al. 1991). In the Wibberenz & Cane (2006) study, it was found that individual events could often be observed at two spacecraft located on field lines with Parker spiral connection points at the Sun that were widely separated, sometimes by more than 80° in heliographic longitude. These authors suggested that some diffusive propagation process in the low corona may be required to explain such events. In contrast, the ^3He studies found that correlated event detections were largely confined to times when the longitudinal separation between the spacecraft were relatively narrow, consistent with the longitudinal spreads inferred from the single-spacecraft studies. One instance was reported (Reames et al. 1991) of a ^3He -rich event which may have been observed by three spacecraft spread over $\sim 60^\circ$ in heliographic longitude, but the data were not sufficient to identify ^3He on one of the spacecraft, allowing for the possibility that they were not all observing the same event.

Using data from the two Solar Terrestrial Relations Observatory (*STEREO*) spacecraft and the *Advanced Composition Explorer* (*ACE*), Wiedenbeck et al. (2010) reported an impulsive event that occurred on 2008 November 3–4 when the *STEREOs* had longitudinal separations of $\pm 41^\circ$ from *ACE*. In this event, ^3He was detected at *STEREO-B* and *ACE* while electrons were detected at all three spacecraft.

In this paper, we summarize the results of a search for additional multispacecraft ^3He -rich SEP events and discuss in detail the event of 2010 February 7, which was detected at both *STEREOs* and *ACE* when the spacecraft spanned 136° in heliographic longitude. We also consider possible causes and consequences of this wide spread.

2. OBSERVATIONS

After having been placed into ~ 1 AU heliocentric orbits around the beginning of 2007, the two *STEREO* spacecraft (launched on 2006 October 25) have been providing SEP measurements that can be used in conjunction with data from *ACE* and other near-Earth spacecraft to obtain multipoint observations of individual SEP events. The *STEREO* orbits are designed such that each of these spacecraft has a separation in heliographic longitude from Earth that increases at a rate of $\sim 22.5 \text{ yr}^{-1}$, with *STEREO-A* leading and *STEREO-B* trailing the Earth.

For the present study, we have used data from the *STEREO* Low Energy Telescope (LET; Mewaldt et al. 2007a), the Suprathermal Ion Telescope (SIT; Mason et al. 2007), and the Solar Electron and Proton Telescope (SEPT; Müller-Mellin et al. 2008), together with *ACE* data from the Ultra-Low-Energy Isotope Spectrometer (ULEIS; Mason et al. 1998), the Solar Isotope Spectrometer (SIS; Stone et al. 1998), and the Electron, Proton, and Alpha Monitor (EPAM; Gold et al. 1998). We performed a systematic search of the *STEREO/LET* data sets for ^3He -rich SEP events occurring between 2007 January when the *STEREOs* and *ACE* were all located near Earth, and 2011 January when the *STEREOs* were leading and trailing the Earth by almost 90° . Since SEP intensities typically decrease with increasing energy, our search for ^3He -rich events relied primarily on ^3He with energies in the range 2.3–3.3 MeV nucleon $^{-1}$, which is just above the *STEREO/LET* energy threshold for this isotope.

Figure 1 shows event-integrated mass histograms from each of the instruments for the 2010 February 7 event, which is discussed in detail below. The identification of ^3He in

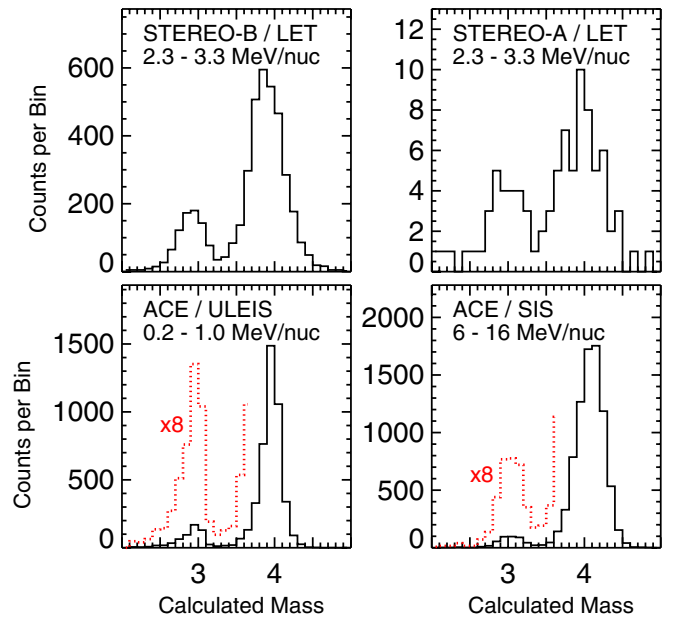


Figure 1. Event-integrated He mass histograms for the 2010 February 7 ^3He -rich solar energetic particle event. Dotted curves (red in the online version) show the ^3He regions of the *ACE* histograms scaled by a factor of eight to better illustrate the isotope separation. Energy intervals are shown for ^3He . For *STEREO/LET*, particles are selected from a specified total energy interval, thus the ^4He energy per nucleon limits are lower than those for ^3He . Similarly, for *ACE/SIS* a specified range interval is used, also resulting in a lower energy per nucleon for ^4He than for ^3He . The *ACE/ULEIS* data are all obtained from a common energy per nucleon interval.

(A color version of this figure is available in the online journal.)

STEREO/LET instruments relies on observing the peak for this isotope in the He mass histogram for particles detected within a given range of *total* energies because the energy per nucleon cannot be calculated until the mass has been determined. In a few cases, the ^3He peak in the histogram for 6.9–9.9 MeV He, which is used to select the 2.3–3.3 MeV nucleon $^{-1}$ ^3He , was obscured by spillover from the ^4He peak. In these cases, the 12.9–24.0 MeV total-energy interval (4.3–8.0 MeV nucleon $^{-1}$ for ^3He) was used to establish the presence of the ^3He -rich event.

Table 1 lists the ^3He -rich SEP events that were detected by one or both of the *STEREO/LET* instruments during the 49 months covered by this study. For each event, the table shows the locations of the two *STEREOs* and indicates which instruments detected the event. Some of the detections are uncertain, as explained in the footnotes. The table shows that detections of the same event by one *STEREO/LET* and by *ACE* are not uncommon, even when the spacing between the two spacecraft is $>60^\circ$. In a few cases, the longitudinal spread of an event is large enough to allow detection at both *STEREOs* and *ACE*, as in the case of two events in 2010 February when the three spacecraft spanned 136° . There were no instances in which an event was detected at both *STEREO* spacecraft but not at *ACE*. This is not surprising because during the time interval studied, the longitudinal separation between the two *STEREO* spacecraft on the Earth-facing side of the Sun ($\equiv \phi_{AB}$) was less than the separation on the opposite side of the Sun ($360^\circ - \phi_{AB}$) and because the *ACE/ULEIS* instrument, which measures ^3He near Earth down to ~ 0.15 MeV nucleon $^{-1}$, is significantly more sensitive to small ^3He -rich events than the *STEREO/LETs*. A number of additional ^3He -rich events that were detected only by *ACE/ULEIS* and not by either *STEREO/LET* were not included in the present study.

Table 1
 ^3He -rich SEP Events Detected by *STEREO-A*/LET or *STEREO-B*/LET from 2007 January Through 2011 January

<i>STEREO</i> Event	Day of Start Date ^a Year	Heliographic Longitudes		^3He -rich Event Detections ^b			
				<i>STEREO-B</i>	<i>ACE</i>	<i>ACE</i>	<i>STEREO-A</i>
		<i>STEREO-B</i>	<i>STEREO-A</i>	LET	ULEIS	SIS	LET
2007 Jan 24 ^c	24	0°	0°	YES	yes	yes	YES
2008 Nov 4 ^c	309	−41°	+41°	YES	yes	no	yes ^d
2009 Apr 29	119	−47°	+47°	no	yes	no	YES
2009 Jul 4	185	−48°	+54°	YES	yes ^e	no	no
2009 Sep 12	255	−55°	+60°	no	no	no	YES
2009 Nov 3	307	−62°	+62°	no	no	yes ^e	YES ^f
2010 Feb 2	33	−70°	+65°	no	no	no	YES
2010 Feb 7 ^g	38	−71°	+65°	YES	yes	yes	yes
2010 Feb 12	43	−71°	+65°	YES	yes ^h	yes ^h	yes
2010 Feb 20	51	−71°	+66°	no	no	no	YES ⁱ
2010 Jun 12	163	−70°	+73°	YES ^j	yes	yes	no
2010 Aug 23	235	−73°	+81°	no	no ^k	no	YES
2010 Aug 31	243	−74°	+81°	no	yes	yes	YES ^l
2010 Oct 20	293	−80°	+83°	no	yes ^m	yes ^m	YES
2010 Nov 2	306	−82°	+84°	no	yes	yes	YES
2010 Nov 11	315	−83°	+84°	YES	no ⁿ	no	no
2011 Jan 21	21	−92°	+86°	YES	yes	no	no

Notes.

^a Start date at the *STEREO*/LET that was used as the basis for identifying the event (typically the one with the higher ^3He fluence). For this *STEREO*, the event detection is indicated with an uppercase “YES” in Column 5 and/or 8. Typical event durations are a few days. Onset times at widely spaced spacecraft can sometimes differ by nearly a day.

^b Some event detections listed as “yes” are uncertain. The associated footnotes explain the reasons.

^c Events discussed by Wiedenbeck et al. (2010).

^d Detection of event on November 4 at *STEREO-A* is uncertain because the intensity was close to the detection threshold. On November 6, a small event was observed at *STEREO-A* only. It is not clear whether it was associated with the *STEREO-B* event of November 4.

^e Weak event close to detection threshold.

^f Increases of ^3He were observed on both November 3 and November 5, but were not well enough separated to analyze as separate events.

^g Event discussed in this paper.

^h At ULEIS and SIS ^3He observed was between February 12 and 19. How much of this activity was associated with the *STEREO-B* event is not clear.

ⁱ February 20 event at *STEREO-A* was weak but ^3He was clearly observed in the 4.3–8.0 MeV nucleon^{−1} energy interval.

^j June 12 event at *STEREO-B* was weak. Spillover from ^4He dominated the ^3He mass region in the 2.3–3.3 MeV nucleon^{−1} interval, but a ^3He peak was observed in the 4.3–8.0 MeV nucleon^{−1} energy interval.

^k During August 23 event, the He at ULEIS was dominated by a CIR. Some ^3He was observed in the 0.4–1.0 MeV nucleon^{−1} energy interval, but timing suggests it was associated with the CIR rather than with the ^3He -rich event observed at *STEREO-A*.

^l Spillover from ^3He interferes with identification of ^3He in 2.3–3.3 MeV nucleon^{−1} interval. Detection based on 4.3–8.0 MeV nucleon^{−1} interval.

^m Multiple ^3He increases observed with ULEIS and SIS between October 17 and 22. It is not clear which of these were associated with the October 20 event observed at *STEREO-A*.

ⁿ A ^3He -rich event was observed by ULEIS starting on November 14, but it appears distinct from the November 11 event detected at *STEREO-B*.

In several cases, the ^3He intensity detected at one or both of the *STEREO*/LETs was only slightly above the background ^3He level. To confirm that the observed ^3He actually was associated with an ^3He -rich SEP event, we used data from other instruments to check for additional signatures of an impulsive event, including enhancements of Fe/O, which are observable with the *STEREO*/SIT and *ACE*/ULEIS, and intensity increases of near-relativistic electrons, which are detected with *STEREO*/SEPT and *ACE*/EPAM.

The first two years of the survey period occurred during the extremely quiet portion of the solar minimum between cycles 23 and 24. Thus, the only events detected with the *STEREO*/LETs were those discussed by Wiedenbeck et al. (2010): a 2007 January event when the three spacecraft were all near Earth and a 2008 November event when the *STEREO*s were 41° from *ACE*. The rate of detection of ^3He -rich events gradually increased through 2009 and 2010, but was still low enough that the occurrence of chance coincidences between detections of ^3He -rich events from widely spaced active regions

was improbable. The study ended in 2011 February when solar activity had started to increase significantly and a combination of higher SEP backgrounds and increased probability of chance associations of events began to complicate the analysis.

In the remainder of this paper, we examine in detail the best-measured three-spacecraft event that was detected. A preliminary discussion of this event has been presented by Wiedenbeck et al. (2011). Figure 2(a) shows ^3He intensity versus time plots for this 2010 February 7 event as observed at *ACE*, *STEREO-A* (leading *ACE* by 65°), and *STEREO-B* (trailing *ACE* by 71°). Figure 2(b) shows the events observed during this period in ~0.07–0.1 MeV electrons, which require ~20 minutes to traverse the nominal 1.2 AU length of a Parker spiral field line between the Sun and 1 AU. From the event onset at *STEREO-B* (indicated approximately by the leftmost arrow on the ^3He plot), it appears that the ^3He was not directly associated with either of the two most prominent electron events, but possibly corresponds to a small inflection seen late on 2010 February 7 in the electron observations from *STEREO-B* and *ACE*. Radio wave

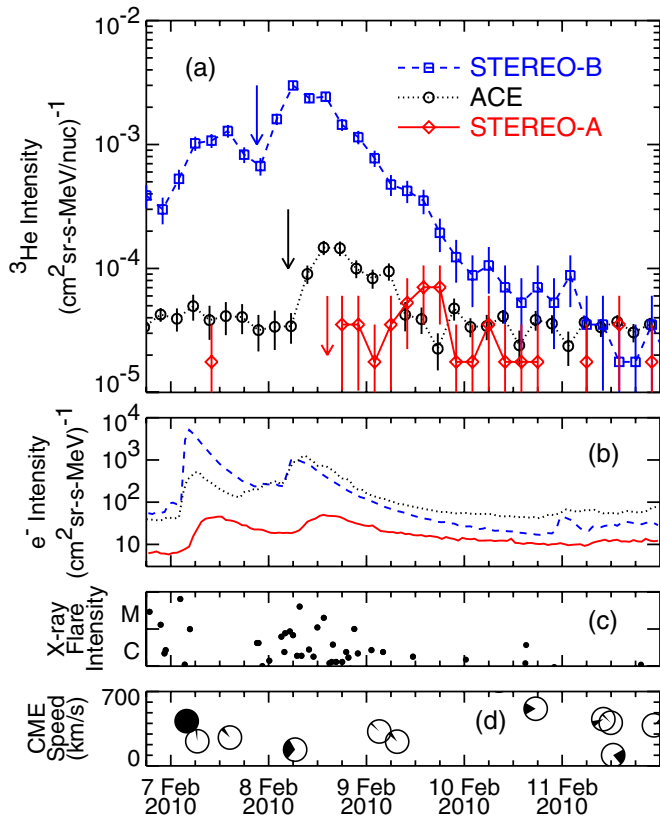


Figure 2. (a) Intensity of ^3He vs. time measured at the three spacecraft. *STEREO* data are LET measurements at energies of 2.3–3.3 MeV nucleon $^{-1}$. *ACE* data are SIS measurements covering 4.6–16.3 MeV nucleon $^{-1}$. Arrows indicate the approximate times of the event onsets. (b) Intensity of ~ 0.07 –0.1 MeV electrons vs. time at the three spacecraft. The *STEREO* data are from the SEPT instruments and the *ACE* data are from the EPAM instrument. (c) X-ray intensity vs. time for identified solar flares of GOES class C1.0 or greater. (d) Measured speed vs. time of occurrence for identified CMEs. Filled wedges indicate the clock angle and the angular width measured for each CME. The filled black circle corresponds to a slow, front-side, halo CME that was the source of an ICME observed at *ACE* on 2010 February 11. The apparent ^3He increase at *STEREO-B* starting around 0000 UT on 2010 February 7 (panel (a)) has not been listed in Table 1 because it includes too much spillover from ^4He to be unambiguously identified as a ^3He -rich event.

(A color version of this figure is available in the online journal.)

observations⁷ from both *STEREOs* and from the *Wind* spacecraft, which was located at the L1 Lagrange point near *ACE*, indicate the occurrence of numerous type III radio bursts during the last $\sim 1/3$ of 2010 February 7, further indicating the escape of electrons from the Earth-facing side of the Sun.

Differences between the ^3He onset times (or peak times) at *STEREO-A* and *STEREO-B* exceed by a factor $\gtrsim 8$ the ~ 2 hr required for ~ 3 MeV nucleon $^{-1}$ ions with 0° pitch angle to traverse the ~ 1.2 AU length of the nominal Parker spiral field line from the Sun to 1 AU. Furthermore, the peak ^3He intensities also differ significantly between the two *STEREO* measurements. The *ACE/SIS* data that are shown correspond to a higher ^3He energy than those from the *STEREO/LETs*, so quantitative comparison of the peak intensity at *ACE* with those observed at the *STEREOs* requires additional analysis.

From Figure 2(c), which shows the times and peak intensities of X-ray flares of GOES class C1.0 or greater compiled by the

Space Weather Prediction Center⁸ (SWPC), it is evident that we are not able to associate the ^3He injection with a specific flare among the large number that were detected. Nevertheless, the location of the injection is reasonably well known because all of the flares during this time period came from the same active region, AR11045, which was located at N23W01 at 0000 UT on 2010 February 8. Inspection of coronal images from *SOHO/EIT* and *STEREO/EUVI* shows that the three C-class flares that occurred after 2100 UT on February 7 were located between E02 and W01, so we determine the injection point to be located at the central meridian to within $\pm 2^\circ$.

Daily active region reports from the SWPC were examined to check for possible sources for an SEP event from the backside of the Sun that could have been the source of the ^3He observed at *STEREO-A*. AR11043, which was at W62 on 2010 February 7, and AR11041, which was last recorded at W58 on 2010 January 31, both had simple (alpha) magnetic configurations with no sunspots. AR11042, which was still producing minor X-ray flares when it rotated past the west limb on 2010 January 27, would have been at \sim E110 at the time of the 2010 February 7 ^3He -rich event, with a connection point at 1 AU lying approximately 125° west of *STEREO-A*. Moreover, *STEREO/EUVI* images of these regions do not show evidence of jets, which have been associated with impulsive SEP events (Wang et al. 2006; Nitta et al. 2008). Thus, we find no plausible alternative to AR11045 as the source for the *STEREO-A* event.

The geometrical arrangement of the three spacecraft, the flare, and selected Parker spiral field lines are illustrated in Figure 3(a). The field lines drawn through the spacecraft locations were calculated using the mean solar wind speed measured during the second half of 2010 February 7 at the respective spacecraft (*STEREO-B*: 480 km s $^{-1}$; *ACE*: 355 km s $^{-1}$; *STEREO-A*: 410 km s $^{-1}$). The field line from the active region (dashed line), which is drawn assuming a speed of 400 km s $^{-1}$, connects to 1 AU at east 60° .

Figure 3(b) shows ^3He fluence spectra for the 2010 February 7 event at each of the spacecraft. The vertical dashed lines indicate the boundaries of the 2.3–3.3 MeV nucleon $^{-1}$ energy interval over which we compare fluences. Although data points from *ACE/ULEIS* and *ACE/SIS* fall below and above this interval, together they provide reasonably good constraints on fluence at these intermediate energies and can be used to obtain the 2.3–3.3 MeV nucleon $^{-1}$ fluence by interpolation, as indicated by the dotted line. Data from the 2007 January 24 ^3He -rich event were previously used to verify the intensity calibrations between the two LETs and the combination of ULEIS and SIS (Wiedenbeck et al. 2010). In Figure 3(c), the resulting 2.3–3.3 MeV nucleon $^{-1}$ averaged fluences are shown as a function of spacecraft heliographic longitude measured from the longitude to which the active region is connected at 1 AU.

The smooth curve, which is the result of a two-parameter Gaussian fit to the three data points with the center of the distribution constrained to lie at the connection longitude, does a reasonable job of representing the measurements. The standard deviation of the Gaussian obtained from the fit is 48° . Varying the assumed center location by 2° results in a change of $\sim 1^\circ$ in the derived width. For comparison, a 13 km s $^{-1}$ change in solar wind speed would also cause a shift of the connection point at 1 AU by $\sim 2^\circ$. The fact that the shape of the observed longitudinal distribution is approximately Gaussian

⁷ secchirh.obspm.fr/swaweb/2010/1002/sur_swaves_20100207_0000_2400.png

⁸ www.swpc.noaa.gov

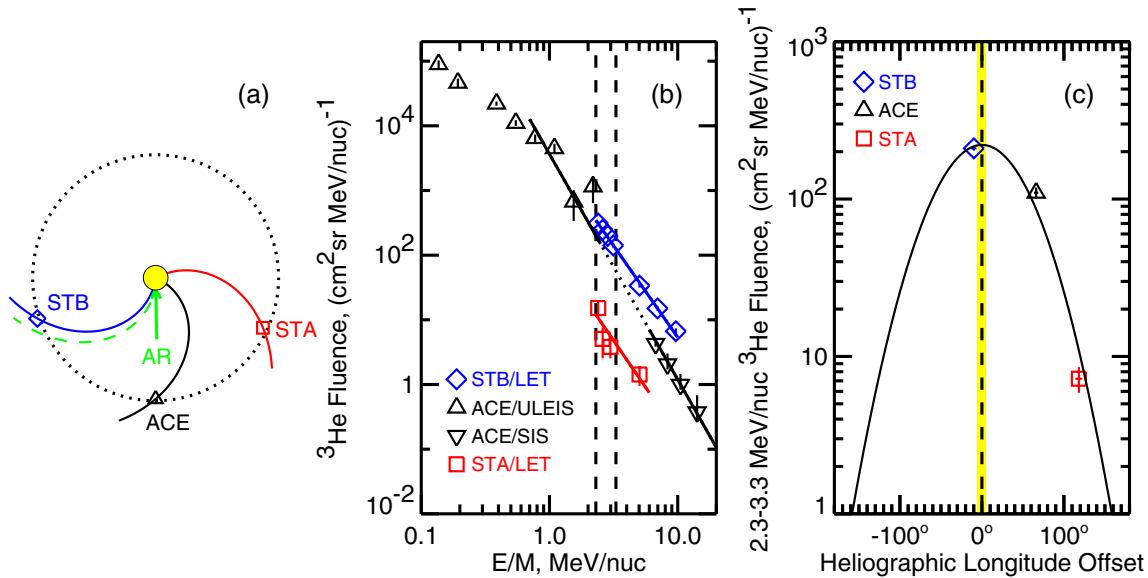


Figure 3. (a) Geometrical arrangement of the *STEREO-B*, *ACE*, and *STEREO-A* spacecraft and the flaring active region at the time of the 2010 February 7 ${}^3\text{He}$ -rich event. The dotted circle corresponds to a radius of 1 AU. (b) Fluence spectra measured at the three spacecraft. Dashed vertical lines indicate the limits of the energy interval used for comparing fluences. Dotted line shows the interpolation between *ACE/ULEIS* and *ACE/SIS* data points used to estimate the fluence at *ACE*. (c) Dependence of measured fluence in the 2.3–3.3 MeV nucleon $^{-1}$ energy interval on heliographic longitude. The abscissa is the longitudinal offset of the spacecraft locations from the 1 AU longitude of the Parker spiral field line that originates at the active region. The solid curve is a Gaussian fit to the three data points, constraining the peak center to be located at the 1 AU connection longitude. Shading (yellow in the online version) about the dashed vertical line indicates the approximate $\pm 1\sigma$ uncertainty in the source location, which is estimated as $\sigma \simeq 19^\circ/\sqrt{12}$, where 19° is the longitudinal extent of the active region.

(A color version of this figure is available in the online journal.)

is suggestive since diffusion from a point source leads to a Gaussian spatial distribution.

3. DISCUSSION

3.1. Origin of the Longitudinal Spread

The observed broad spread of ${}^3\text{He}$ in heliographic longitude is not expected from the simple model commonly used to describe the release of energetic particles from impulsive SEP events. In this model (Shimojo & Shibata 2000; Reames 2002), closed field lines in an active region undergo reconnection with adjacent open field lines so that some of the particles accelerated in the reconnection event have access to the heliosphere along these open field lines. Because of the small size of the reconnection region, one expects that the open field will span a relatively small range of angles as it expands into the heliosphere.

The rate of particle diffusion perpendicular to the mean magnetic field, which could result from cross-field scattering, field-line random walk, or a combination of both effects, is not tightly constrained but under normal conditions it is expected to be much smaller than parallel diffusion (e.g., Dröge et al. 2010). Interruptions in the intensity of impulsive SEP events lasting several hours are sometimes observed at 1 AU. These “dropouts” (Mazur et al. 2000) are attributed to convection past the observer of successive magnetic flux tubes with different connection points at the Sun such that some have been populated with particles from an impulsive event and others have not. The existence of these relatively sharp boundaries between different particle populations suggests that cross-field diffusion is not responsible for transport over a large range of heliographic longitudes in these events. Dröge et al. (2010) found that the ratio between perpendicular and parallel diffusion coefficients required to account for such dropouts is $\kappa_{\perp}/\kappa_{\parallel} \lesssim 10^{-4}$.

Using observations included in our preliminary report of the 2010 February 7 event (ACE News #137⁹), Giacalone & Jokipii (2012) attempted to account for the observed characteristics using an interplanetary transport model and found that reasonable agreement could be obtained by assuming parallel scattering mean free paths of a few tenths of an AU and $\kappa_{\perp}/\kappa_{\parallel} \simeq 10^{-2}$. These authors point out that large longitudinal spreads and the presence of dropouts do not need to be mutually exclusive since it is possible that the longitudinal spreading could result from the field line random walk associated with footpoint motions at the photosphere rather than from cross-field scattering of particles in the interplanetary medium. Furthermore, since dropouts were not observed in the February 7 event, significant cross-field scattering is not ruled out by the data. However, lacking an independent measure of the interplanetary scattering conditions, we are unable to test whether the conditions assumed by Giacalone & Jokipii (2012) actually existed. Thus, we also considered other possible causes for the longitudinal spread.

It is well established that field lines from an active region can undergo significant spreading, and possibly displacement, between the solar photosphere and the “source surface” at which the field becomes radial and opens out into the heliosphere (e.g., Liewer et al. 2004). The fact that the 2010 February 7 event, which originated from an active region at N23, was observed in the ecliptic plane suggests that at least this amount of angular (latitudinal) displacement occurred between the photosphere and the source surface, assuming that perpendicular diffusion effects were not responsible for the latitudinal transport. Potential field source surface (PFSS) models (e.g., Schrijver & DeRosa 2003) have had some success in describing coronal fields (e.g., Liewer et al. 2004). However, attempts to trace flows of energetic electrons (Rust et al. 2008) or ions (Nitta et al. 2006)

⁹ www.srl.caltech.edu/ACE/ACENews/ACENews137.html

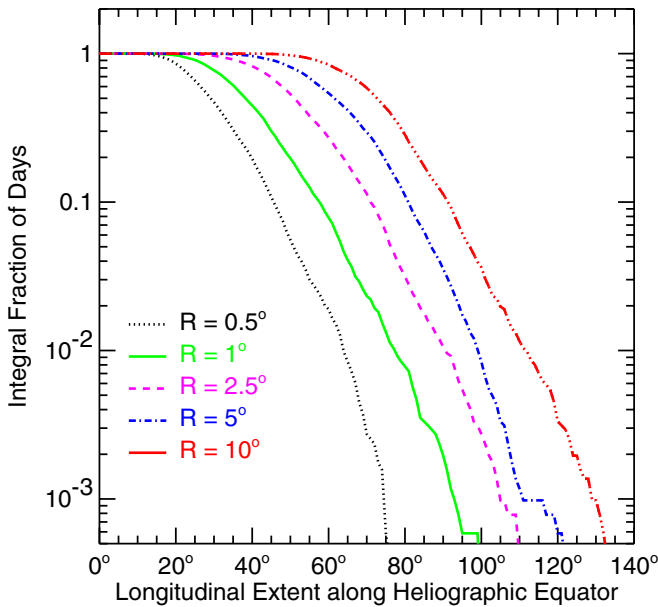


Figure 4. Integral distributions of longitudinal size, in number of degrees along the heliographic equator, for the largest cluster of field lines identified in PFSS model maps for each day over a 14 year period extending from 1998 through 2011. Here, a cluster is defined as consisting of those field lines originating within a radius R at the solar photosphere and mapping to the heliographic equator on the source surface. Curves show the fraction of days when the largest longitudinal spread was greater than the value given by the abscissa. Curves correspond to five different criteria for the cluster radius at the photosphere, as indicated in the legend. For comparison, the separation between *STEREO-A* and *STEREO-B* at the time of the 2010 February 7 was 136° .

(A color version of this figure is available in the online journal.)

from a solar flare site to 1 AU using the PFSS model field in the corona and a Parker spiral field in the heliosphere have had $\lesssim 50\%$ success. Klein et al. (2008) investigated several electron events in which the longitudinal transport was consistent with as much as 50° field-line displacement between an active region and the source surface, as predicted by calculations. We have examined PFSS estimates of the coronal field at the time of the 2010 February 7 ^3He -rich event using information available from SolarSoft¹⁰ and from the GONG Web site.¹¹ Although there are significant differences between maps intended to represent the same field, a consistent feature is that in each map field lines originating near AR11045 and reaching the source surface near the solar equatorial plane encompass a wide range of heliographic longitudes, but that range is nevertheless $\lesssim 2/3$ the longitudinal separation between the two *STEREOs*.

To further check on the possibility that magnetic field expansion between the photosphere and the source surface could, at times, produce a longitudinal spread as large as the 136° we observe, we have examined daily PFSS maps covering a 14 year time interval (1998 through 2011). For each map, field lines reaching the source surface along the heliographic equator were traced back to their points of origin at the photosphere and instances in which a large number of these field lines were rooted within a specified angular radius, R , of one another were identified. Among the various field line “clusters” that were found for a given day, the one with the largest longitudinal spread at the source surface was selected. Figure 4 shows integral distributions of these largest cluster longitudinal spreads for several

different values of R . Each curve is based on ~ 5100 PFSS daily maps covering more than a full solar cycle. As seen from these distributions, spreading of field lines originating within a radius $\leq 10^\circ$ at the photosphere to cover as much as 136° (the separation between the two *STEREOs* at the time of the 2010 February 7 event) along the heliographic equator must be regarded as an extremely rare occurrence. Thus, we find it unlikely that spreading of the magnetic field in the corona could have been the main contributor to the observed longitudinal width of this event.

It is known that impulsive SEP events are sometimes accompanied by CMEs (Kahler et al. 2001; Nitta et al. 2006), although often these CMEs are too slow to drive a shock that would accelerate particles. Indeed, in the case of the 2010 February 7 event, there was no fast CME observed and also no evidence for a shock, either in the form of a type II radio burst or an in situ detection of shock signatures.

However, a flaring active region can produce a sequence of SEP events and CMEs and thus it is not uncommon to have SEPs from a ^3He -rich event released into an environment that has experienced the launch of one or more CMEs within the preceding several days. Such CMEs can distort the magnetic field and possibly lead to reconnection that further alters the field geometry and the paths of subsequently released particles. Figure 2(d) indicates the speeds and detection times of identified CMEs.¹² Of particular note is the halo CME shown around 0400 UT on 2010 February 7, which has been identified¹³ as the source of an interplanetary CME (ICME) detected at *ACE* starting around 0800 UT on 2010 February 11. The leading edge of this $\sim 421 \text{ km s}^{-1}$ CME, which was directed generally toward Earth, would have been at $\sim 0.15\text{--}0.2$ AU at the release time of the 2010 February 7 ^3He -rich event and thus could have been in a position to significantly influence the large-scale distribution of particles released behind it. Determining whether such preceding CMEs play a crucial role in causing the large longitudinal spreads observed in some ^3He -rich SEP events will require a future statistical study including additional ^3He -rich events.

There have been a number of reports of “sympathetic flares” (see Schrijver & Title 2011 and references therein) in which two solar flares are observed at well separated locations on the Sun with small enough differences in their times of occurrence that a causal connection appears probable. In one example of this type, Schrijver & Title (2011) report evidence for magnetic separatrices connecting distant sites of activity and conclude that the evolution of the field at one location can be “essential to the evolution, and possibly even to the initiation, of the flares and eruptions over an area that spans at least 180° in longitude.” Thus, it is possible that sympathetic flares could lead to nearly simultaneous ^3He -rich events that can be observed at widely separated longitudes in the heliosphere. However, in the 2010 February 7 event, there was no good candidate active region with a complex magnetic configuration near the nominal connection point of *STEREO-A* that would provide a likely source for a sympathetic flare that could be triggered by the activity at AR11045. In addition, the *STEREO/EUVI* data did not show evidence for flares or jets in this region of the corona. It should be noted, however, that Mason et al. (2009) reported a few instances in which ^3He -rich SEP events were observed when a single, magnetically simple western-hemisphere active region

¹⁰ www.lmsal.com/~derosa/pfsspack

¹¹ gong.nso.edu/data/magmap/QR/bq5

¹² cdaw.gsfc.nasa.gov/CME_list/UNIVERSAL/univ2010_02.html

¹³ www.srl.caltech.edu/ACE/ASC/DATA/level3/icmetable2.htm

was the only candidate source, but no detectable X-ray flare and only minor brightenings in the EUV were observed.

Another mechanism that could lead to a causal connection between flares at widely separated locations involves wave propagation from a coronal disturbance caused by one flare to a remote site where it can destabilize the field and trigger a subsequent event (Krucker et al. 1999). *STEREO*/EUVI data do show some large-scale disturbances (“EIT waves”) in connection with several flares that occurred during February 7–8, but they did not occur during the time range of interest, late on February 7.

Recent work on the origin of the slow solar wind (Antiochos et al. 2011; Edmondson 2011 and references therein) has considered a puzzle similar to that posed by the wide longitudinal spread we are finding in impulsive SEP events. The slow wind, with its composition similar to that of closed-field regions in the corona, is thought to be released by means of reconnection at the boundary between open and closed field regions, yet the slow wind extends over a much wider range in heliographic latitude than does this boundary region. Calculations discussed by Antiochos et al. (2011) indicate that distinct open field regions are connected by narrow open-field corridors that map into a web of separatrices and quasi-separatrix layers in the heliosphere that extends far from the heliospheric current sheet and provides widely distributed source regions that can contribute to the slow solar wind. There is a possibility that an extensive network of open-field regions of the sort envisioned by these authors could, at times, provide a mechanism for energetic particle transport over a wide range of heliographic longitudes. Although further model calculations would be needed to explore the plausibility of this suggestion, it is conceivable that energetic particle transport could provide a useful means for probing these complex magnetic structures.

3.2. Additional Constraints

There are additional observational constraints that should help distinguish among the possible mechanisms for producing impulsive SEP events with wide longitudinal spreads. As noted above, both the ^3He time–intensity profiles and total fluences differ significantly between the three observing spacecraft in the 2010 February 7 event (Figures 2 and 3). As shown by Giacalone & Jokipii (2012), these characteristics can be explained as results of interplanetary diffusion with appropriate choices of the parallel and perpendicular diffusion coefficients. If the longitudinal width were caused by a mechanism such as field line spreading between the photosphere and the source surface, in which accelerated particles are directly injected on field lines that expand to cover a wide range of heliographic longitudes, then it would appear more difficult to produce large differences in the event characteristics at different locations, at least if the parallel mean free path is a significant fraction of an AU. However, if particles were not directly injected onto a cluster of field lines as a result of the acceleration event, but rather had to diffuse over some distance in the corona to populate the field lines, then it may be possible to produce event characteristics very similar to those obtained from models involving interplanetary diffusion. Such coronal diffusion scenarios have previously been proposed (e.g., Wibberenz & Cane 2006 and references therein).

The organization of measured ^3He fluences as a monotonic function of distance from the heliographic longitude that is best connected to the source region (Figure 3(c)) may also be useful for distinguishing among candidate explanations for

the longitudinal spreading. For example, to produce such a pattern by diffusion in the corona, one would expect that the one-dimensional ordering of field lines along the ecliptic plane would need to map monotonically into a one-dimensional array of footpoints at the photosphere. Thus, if a similar monotonic pattern of fluences at 1 AU turns out to be a common feature of impulsive events, then it would be useful to investigate how the field lines map back to the photosphere in PFSS models.

If broad longitudinal distributions of fluences were associated with disturbances of the coronal and/or heliospheric fields by CMEs preceding the ^3He -rich events, then these distributions could vary significantly from event to event. A study of additional ^3He -rich events should help clarify the range over which the width of the fluence distributions can vary and aid in identifying correlations with parameters upon which the width may depend (e.g., the presence of preceding CMEs).

Patterns of successive events at widely separated spacecraft may provide additional constraints. For this purpose, the near-relativistic electron events that often accompany ^3He -rich events can be particularly useful since they have a sharper, better defined time structure than the few-MeV nucleon $^{-1}$ ^3He . For example, as seen in Figure 2, the ^3He -rich event with onset late on 2010 February 7 occurred between two well-defined electron increases. If these events all originated within a span of less than two days from the same active region, then it would not be surprising to find that the particles had access to a similar range of heliographic longitudes. If, on the other hand, these events were due to sympathetic flares in which an event at one location triggered a separate event at a distant location, then it would be necessary to assume that the magnetic topology responsible for the sympathetic flaring must have persisted in a state such that the triggering process could be activated multiple times in spite of any changes that may have resulted from the flare-associated reconnection.

3.3. Comparison with Single-spacecraft Study Results

The substantially broader width of the fluence distribution shown in Figure 3(c) than the distribution of flares locations associated with ^3He -rich SEP events detected at a single spacecraft at 1 AU (Reames 1999) may be attributable to the instrumental sensitivity threshold for detecting ^3He . Because the fluence decreases significantly with separation from the longitude best connected to the flare site, ^3He -rich events with fluence close to the instrument threshold will only be detected when the observer is near the well connected longitude, thus narrowing the longitude distribution of the associated flares. A quantitative formulation of this effect is presented in the Appendix.

3.4. Relationship to Other ^3He Observations

The broad width over which ^3He -rich events are sometimes observed and the strong dependence of the ^3He fluence on the separation from the heliographic longitude that is well connected to the source region may provide insight into several previously reported characteristics of such events.

Using the width of the longitudinal distribution of X-ray flares associated with ^3He -rich events, Reames (1993, 1999) scaled the number of observed events to obtain an estimate of ~ 1000 per year for the number of ^3He -rich events on the visible disk of the Sun at solar maximum. The present study suggests that a combination of the instrument sensitivity and the distribution of event fluences at the well-connected longitude must play an important role in determining the interval of

heliographic longitudes over which events can be observed. Thus, the Reames (1993, 1999) estimate could be subject to a sizeable systematic bias that depends on the instrument and the event identification criteria that were employed. At present, we cannot rule out the possibility that the event size distribution could be dominated by a large number of events too small to be detected with the present instrumentation. As noted above, data from the *ACE/ULEIS* instrument, which is particularly sensitive to ^3He -rich events due to its energy coverage down to ~ 0.15 MeV nucleon $^{-1}$ and its good He isotope resolution, reveal a number of events that were not detectable above the higher energy thresholds of the *ACE/SIS* and *STEREO/LET* instruments.

Wiedenbeck et al. (2003, 2005) used data from *ACE/ULEIS* and *SIS* to study the fraction of time that energetic ^3He associated with impulsive SEP events was observed in the interplanetary medium near 1 AU. The average value exceeded 50% over most of the 1999–2003 solar maximum, with the fraction exceeding 90% during several solar rotations. If the analysis is restricted to *SIS* energies ($\gtrsim 5$ MeV nucleon $^{-1}$), then the fraction is a factor ~ 2 – 3 less, presumably due to a combination of the soft energy spectra in many ^3He rich events (Mason et al. 2002) and the possibility of detecting events over a broader range of heliographic longitudes by taking advantage of the *ULEIS* sensitivity below 1 MeV nucleon $^{-1}$.

In studies that have attempted to associate specific X-ray flares with detected ^3He -rich SEP events, it is not uncommon to find events with no clear X-ray counterpart near the expected release time from the Sun (e.g., Nitta et al. 2006). It may be that in some of these cases, ^3He from a flare on the backside of the Sun is reaching the observer because of the large spread of the particles in heliographic longitude. With a nominal Parker spiral for a solar wind speed of 400 km s $^{-1}$, an event on the west limb will have a connection point at 1 AU that is only $\sim 30^\circ$ west of the observer. This separation is less than the 1σ width of the fluence distribution plotted in Figure 3(c). It is possible that when ^3He is detected from a backside flare, accidental coincidence with another X-ray flare on the visible side of the Sun could result in misidentification of the source location, thus leading to outliers in the distribution of associated flare longitudes (e.g., source locations east of central meridian). The relatively long delays in the onsets of ^3He -rich SEP events detected at large separations from the well-connected longitude (e.g., Figure 2(a)) may also contribute to difficulties in identifying associated X-ray flares.

4. SUMMARY AND CONCLUSIONS

The distribution in heliographic longitude of energetic ^3He from impulsive SEP events has been studied using data from energetic particle instruments on the two *STEREO* spacecraft and on *ACE* as the range of longitudes spanned by the three spacecraft increased from 0° to nearly 180° during the solar minimum period between 2007 January and 2011 January. Multispacecraft detections of ^3He from individual events were not uncommon, even when the *ACE*-to-*STEREO* spacings were $>60^\circ$. In the 2010 February 7 event, which is the best example observed to date of an event in which ^3He was detectable at three widely spaced spacecraft (136° longitudinal separation between the two *STEREO*s), the ^3He fluence was found to have a strong dependence on separation from the heliographic longitude connected to the source region, differing by a factor >30 between the two *STEREO*s. In this event, fluence as a function of heliographic longitude was found to be well fitted

by a Gaussian with standard deviation $\sim 48^\circ$ centered at the best-connected longitude.

Previous results indicating that X-ray flares associated with ^3He -rich SEP events have a relatively narrow distribution in heliographic longitude (Reames 1993, 1999) may be reconcilable with the present work by taking into account the effects of instrument sensitivity thresholds for ^3He detection in conjunction with the strong dependence of fluence on longitudinal separation from the field line connected to the source region. The wide longitudinal spread of ^3He -rich SEP events may also be relevant to issues such as the frequency with which suprathermal ^3He is present as seed material for acceleration by coronal and interplanetary shocks.

The physical mechanism responsible for the broad spread in heliographic longitude is, at present, not clearly established. Several possible mechanisms have been considered and found to merit examination in a future statistical study of ^3He -rich events using multispacecraft observations. It has been found that interplanetary diffusion perpendicular to the mean magnetic field can do a reasonable job of reproducing the ^3He observations if a sufficiently large value of $\kappa_\perp/\kappa_\parallel$ is assumed (Giacomini & Jokipii 2012), but at present we do not have an independent test of whether κ_\perp had a large enough value at the time of the February 7 event. If interplanetary diffusion turns out to be a major contributor to the longitudinal spreading of energetic particles in impulsive SEP events, then multispacecraft observations of the particle distributions may provide a useful probe of scattering conditions in the interplanetary medium.

The longitudinal spreading of magnetic field lines between their photospheric footpoints near an active region and the equatorial plane at the source surface must be considered. Although we find that this mechanism rarely produces longitudinal spreads as broad as the 136° separation of the *STEREO*s on 2010 February 7, it frequently leads to spreads sufficient to explain many of the ^3He -rich SEP events that we have observed at two spacecraft (Table 1).

Finally, the effects of distortion or reconnection in the large-scale coronal and/or heliospheric magnetic fields deserves additional study. Particle propagation in the 2010 February 7 event might have been influenced by a slow, halo CME that occurred ~ 1 day earlier and resulted in an ICME that was detected at Earth several days later. Finally, it must be acknowledged that the longitudinal spreading of energetic particles in ^3He -rich events may be due to a combination of these effects and that the dominant cause could differ from one event to the next. Future statistical studies should help clarify the relative importance of the various physical mechanisms.

We thank Justin Edmondson for his comments on the possible relationship between our results and recent work on the origin of the slow solar wind. Information on CMEs was obtained from the catalog generated and maintained at the CDAW Data Center by NASA and The Catholic University of America in cooperation with the Naval Research Laboratory. This work was supported by NASA at Caltech (under grants NNX08AI11G, NNX10AQ68G, and NNX10AQ68G, and through UC Berkeley under contract NAS5-03131), JPL, APL (under grant NNX10AT75G), and LMSAL (under grants NNX07AN13G and NNX08AB23G). The *STEREO/SEPT* work was supported under grant 50 OC 0902 by the German Bundesministerium für Wirtschaft through the Deutsches Zentrum für Luft- und Raumfahrt (DLR).

APPENDIX

SENSITIVITY EFFECTS ON FLARE
LONGITUDE DISTRIBUTION

As mentioned in Section 3.4, the strong dependence of ${}^3\text{He}$ fluence on the observer's longitudinal separation from the field line that is best connected to the solar source can lead to a bias in the derived longitudinal distribution of a solar indicator of the source location such as X-ray flares. Using S_0 to denote the ${}^3\text{He}$ fluence at the best-connected longitude, we write the distribution of this quantity as $f(S_0)$, which we assume to be independent of heliographic longitude when averaged over a long period of time. Using $g(\phi)$ to denote the dependence of fluence on longitudinal separation, ϕ , from this best-connected longitude, an observer at this separation would observe a fluence $S = S_0 g(\phi)$. If the ${}^3\text{He}$ fluence measurement has a finite detection threshold, S_{thresh} , then the number of ${}^3\text{He}$ -rich events that would be detected with a longitudinal separation of between ϕ and $\phi + d\phi$ will be $N(\phi) d\phi$, with

$$N(\phi) = \int_{S_{\text{thresh}}/g(\phi)}^{\infty} f(S_0) dS_0. \quad (\text{A1})$$

Taking $g(\phi)$ to be a Gaussian with standard deviation σ as observed in the 2010 February 7 event (i.e., $g(\phi) \propto \exp[-\phi^2/2\sigma^2]$) and the event size distribution to be a power law with index $-\alpha$ (i.e., $f(S_0) \propto S_0^{-\alpha}$ with $\alpha > 1$), Equation (A1) gives

$$\begin{aligned} N(\phi) &\propto \int_{S_{\text{thresh}}/g(\phi)}^{\infty} S_0^{-\alpha} dS_0 \propto g(\phi)^{\alpha-1} \\ &\propto \exp[-\phi^2/2(\sigma/\sqrt{\alpha-1})^2]. \end{aligned} \quad (\text{A2})$$

That is, the distribution of detected source longitudes is a Gaussian with standard deviation $\sigma/\sqrt{\alpha-1}$, which for $\alpha > 2$ is narrower than the Gaussian characterizing the dependence of fluence on longitude. Although the assumed threshold, S_{thresh} , affects the total number of detected ${}^3\text{He}$ -rich events, in the special case where the event size distribution is a power law, it does not affect the shape of the derived source location distribution.

Comparison of the width of the two measured Gaussian distributions (fluence versus longitude and source location versus longitude) could, in principle, provide information about the exponent of the power-law fluence distribution (or of a power-law approximation evaluated near the fluence sensitivity

threshold in the case of a more general event-size distribution), this exercise is hindered by several facts. First, the derived flare longitude histogram is, in all likelihood, broadened by variations in the solar wind speed and, second, the longitudinal distribution of the fluence may not be well characterized by the measurements in the 2010 February 7 event, which is one of the few events that have been detected at all three spacecraft.

REFERENCES

- Antiochos, S. K., Mikić, Z., Titov, V. S., Lionello, R., & Linker, J. A. 2011, *ApJ*, **731**, 112
- Dröge, W., Kartavykh, Y. Y., Klecker, B., & Kovaltsov, G. A. 2010, *ApJ*, **709**, 912
- Edmondson, J. K. 2011, *SSRv*, **172**, 209
- Giacalone, J., & Jokipii, J. R. 2012, *ApJL*, **751**, 53
- Gold, R. E., Krimigis, S. M., Hawkins, S. E., et al. 1998, *SSRv*, **86**, 541
- Kahler, S. W., Reames, D. V., & Sheeley, N. R. 2001, *ApJ*, **562**, 558
- Klein, K.-L., Krucker, S., Lointier, G., & Kerdran, A. 2008, *A&A*, **486**, 589
- Krucker, S., Larson, D. E., Lin, R. P., & Thompson, B. J. 1999, *ApJ*, **519**, 864
- Liewer, P. C., Neugebauer, M., & Zurbuchen, T. 2004, *SoPh*, **223**, 209
- Mason, G. M., Gold, R. E., Krimigis, S. M., et al. 1998, *SSRv*, **86**, 409
- Mason, G. M., Korth, A., Walpole, P. H., et al. 2007, *SSRv*, **136**, 257
- Mason, G. M., Nitta, N. V., Cohen, C. M. S., & Wiedenbeck, M. E. 2009, *ApJL*, **700**, 56
- Mason, G. M., Wiedenbeck, M. E., Miller, J. A., et al. 2002, *ApJ*, **574**, 1039
- Mazur, J. E., Mason, G. M., Dwyer, J. R., et al. 2000, *ApJL*, **532**, 79
- Mewaldt, R. E., Cohen, C. M. S., Cook, W. R., et al. 2007a, *SSRv*, **136**, 285
- Mewaldt, R. E., Cohen, C. M. S., Mason, G. M., et al. 2007b, *SSRv*, **130**, 207
- Müller-Mellin, R., Böttcher, S., Falenski, J., et al. 2008, *SSRv*, **136**, 363
- Nitta, N. V., Mason, G. M., Wiedenbeck, M. E., et al. 2008, *ApJL*, **675**, 125
- Nitta, N. V., Reames, D. V., DeRosa, M. L., et al. 2006, *ApJ*, **650**, 438
- Reames, D. V. 1996, *AdSpR*, **13**, 331
- Reames, D. V. 1999, *SSRv*, **90**, 413
- Reames, D. V. 2002, *ApJL*, **571**, 63
- Reames, D. V., Dennis, B. R., Stone, R. G., & Lin, R. P. 2002, *ApJ*, **327**, 998
- Reames, D. V., Kallenrode, M.-B., & Stone, R. G. 1991, *ApJ*, **380**, 287
- Reames, D. V., & Stone, R. G. 1986, *ApJ*, **308**, 902
- Rust, D. M., Haggerty, D. K., Georgoulis, M. K., et al. 2008, *ApJ*, **687**, 635
- Schrijver, C. J., & DeRosa, M. L. 2003, *SoPh*, **212**, 165
- Schrijver, C. J., & Tittle, A. M. 2011, *JGR*, **116**, A04108
- Shimojo, M., & Shibata, K. 2000, *ApJ*, **542**, 1000
- Stone, E. C., Cohen, C. M. S., Cook, W. R., et al. 1998, *SSRv*, **86**, 357
- Wang, Y.-M., Pick, M., & Mason, G. M. 2006, *ApJ*, **639**, 495
- Wibberenz, G., & Cane, H. V. 2006, *ApJ*, **650**, 1199
- Wiedenbeck, M. E., Mason, G. M., Christian, E. R., et al. 2003, in AIP Conf. Proc. 679, Solar Wind Ten: 10th Proc. Int. Solar Wind Conference, ed. M. Velli et al. (Melville, NY: AIP), 652
- Wiedenbeck, M. E., Mason, G. M., Cohen, C. M. S., et al. 2005, in Proc. 29th Int. Cosmic Ray Conf. (Pune), vol. 1, 117
- Wiedenbeck, M. E., Mason, G. M., Cohen, C. M. S., et al. 2011, in Proc. 32nd Int. Cosmic Ray Conf. (Beijing), vol., 10, 205
- Wiedenbeck, M. E., Mason, G. M., Gómez-Herrero, R., et al. 2010, in AIP Conf. Proc. 1216, 12th Int. Solar Wind Conf., ed. M. Maksimovic et al. (Melville, NY: AIP), 621